New synthetic fluid dynamic model for aerospace four-ways servovalve

ISSN 1590-8844
International Journal of Mechanics and Control, Vol. XX, No. 0Y, 20ZZ

NEW SYNTHETIC FLUID DYNAMIC MODEL FOR AEROSPACE FOUR-WAYS SERVOVALVE

Matteo D. L. Dalla Vedova* Pier Carlo Berri* Cosimo Corsi* Parid Alimhillaj**

* Department of Mechanical and Aerospace Engineering, Politecnico di Torino

** Department of Energy, Faculty of Mechanical Engineering, Polytechnic University of Tirana

ABSTRACT

Design and development of modern flight control systems require highly detailed computer models of the on-board equipment in order to emulate its behaviour; conversely, simplified models are needed in preliminary design optimization and diagnostic or prognostic strategies. In these cases constrains on computational time require to implement simplified models able to combine sufficient levels of accuracy and reliability with reduced computational costs. In this context, this work proposes a new simplified numerical model of the servovalve fluid-dynamic behaviours; this algorithm, characterized by a semi-empirical formulation, account for the effects of spool geometry, variable supply pressure and water hammer. In order to evaluate the approximations introduced by this model into a system-level simulation, it has been integrated in a proper numerical model emulating the behaviour of a typical electrohydraulic on-board actuator. It is compared with a higher fidelity servovalve model and its accuracy is evaluated both regarding the static pressure-flow characteristic and servomechanism dynamic response.

Keywords: EHA, Fluid dynamic numerical model, Lumped parameters, Non-linear numerical model, Servovalve

1 INTRODUCTION

Modern flight control systems are characterised by a growing number of increasingly complex components; their design aims to meet increasingly severe requirements in terms of performance and safety levels. From the design point of view, it implies the need for highly detailed models to analyse specific components or subsystems. On the contrary, simpler and more synthetic models are required, despite having an acceptable level of accuracy, for the simulation of the dynamic behaviour of entire systems, in particular in the case of high workload relative to computers when monitoring activities must be performed. The synthetic models mentioned above are particularly suitable for system monitoring software, generally used both on the ground and in flight.
This task must be performed in real-time, so it requires a high burden for the onboard computers. The above considerations can be applied to the primary component of any proportional hydraulic control system, i.e. hydraulic control valves, sequence valves, counterbalance valves, shut-off valves, servovalves (SVs), electrohydraulic or hydromechanical actuators, etc.

2 AIMS OF THE WORK

In this work, the authors consider a typical on board electrohydraulic actuator (EHA) architecture. Specifically, we refer to a four-ways control valve (supply port S, return port R, control port 1, control port 2) coupled with a symmetrical linear jack, as shown in Figure 1. We aim at obtaining a computationally light model for prognostic applications [1], and focus in particular on the second stage sliding spool valve, as its highly nonlinear behaviour accounts for most computational burden of high-fidelity, CFD-based models [2-6]. In addition, it has been shown that strong linearity assumptions on the spool operation may noticeably degrade the accuracy of the whole servoactuator model in some operating conditions [7, 8].

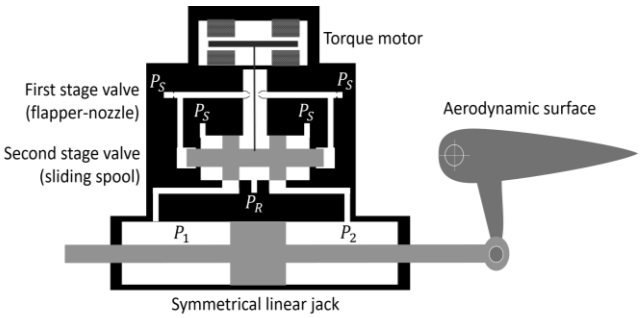

Figure 1 Schematic cross section of a typical electrohydraulic actuator (EHA).

3 CONSIDERED NUMERICAL TEST BENCH

As reported in [9], any fluid-dynamic control valve types can be classified in one of the following two categories:

- models with controlled differential pressure acting on the motor as an output;
- models with controlled output flow.

The first category describes the relationship between an output variable that is considered as the differential pressure imposed on the motor element and an input variable represented by the displacement of the spool, having as feedback the flow controlled through the motor element itself. This consideration is quite valid both in the highly detailed models [10] and in the simplified ones, which will be considered in this work. Conversely, the second category of models, which will not be dealt with in the present work, has the flow controlled as an output variable and the differential pressure as a feedback input, while the displacement of the SV regulating spool is still maintained as the primary input variable.

As previously introduced, in this paper authors considered the first category of simplified fluid-dynamic numerical model (SFNMs), referring to a four-ways type control valve (named respectively supply port *S*, return port *R*, control port *1*, control port *2*), coupled with a linear jack through the two control ports [9].

As schematically represented in Fig. 1, the valve spool displacement x_S rules the opening and closing of the four passageways, each characterized by its overlaps or underlap, to connect each control port either to the supply or return port. This allows to provide the desired relationship between flow and absolute pressure for each control port (P_1 and P_2), for given oil characteristics [11-12].

The corresponding differential pressure, regulated between the two control ports is $P_{12} = P_1 - P_2$. In zero-flow conditions, each control port absolute pressure is close to the supply or return pressure when the corresponding passageway is completely opened.

When the spool is in an intermediate position, the control port pressures have a progressive evolution between return pressure (P_R) and supply pressure (P_S) values, as it can be seen in the valve characteristic P_{12} - x_S of Fig. 2.

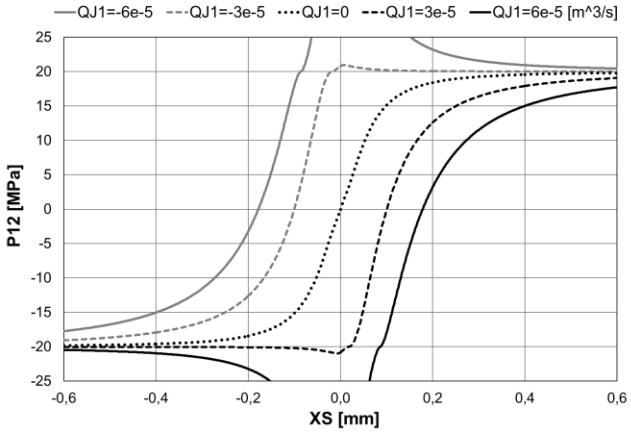

Figure 2 Differential pressure - spool position valve characteristic P_{12}-X_S (HD fluid dynamic model).

Here, the P_{12} - x_S curve is reported for different values of the jack flow Q_J; these data have been obtained with a high fidelity (HF) numerical simulation model, accounting for the actual pressure drops caused by the restricted passages of the valve, implemented in FORTRAN and Matlab-Simulink, and validated by comparison with certified numerical codes and experimental data [13-21].
It should be noted that, from a computational point of view, the HF model is quite burdensome and time-consuming; besides, it is highly dependent on various parameters relating to the SV geometry and the physical characteristics of the hydraulic fluid. Moreover, we must take into account the fact that many of these variables are often not directly available or cannot be measured with adequate precision.
Therefore, it is usually adopted a more straightforward, lighter and faster approach, in which the controlled differential pressure between the two control ports P_{12} and the single flow value Q_J (common to both control ports) are calculated with linearized models.

4 PREVIOUS SIMPLIFIED VALVE MODELS

The most common simplified servovalve models available in the literature simulate fluid-dynamic behaviour through a linearized approach, based on two coefficients that can be easily measured experimentally; these coefficients are the pressure gain (G_P) and the flow gain (G_Q) [9] (see Fig. 3).
This simplified model can be expressed as follows:

$$P_{12} = G_P\,(x_S - Q_J / G_Q) \qquad (1)$$

The displacement of the SV spool produces a proportional value of the differential pressure, which acts on the motor element (i.e. the linear actuator). This displacement is reduced by the pressure loss caused by the oil flow passing through the regulating passages; this counterpressure effect is evaluated in the model through the flow gain. The main drawback of this approach is its inability to assess the pressure saturation due to the limited supply value and the actual stall conditions of the motor element.

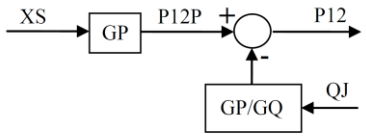

Figure 3 Linearized SV fluid-dynamics numerical model.

It must be noted that this linearized numerical model is not able to take into account the effects due to the maximum value of differential pressure P_{SR} provided by the hydraulic supply or to an eventual pressure supply drops (e.g. a partial depressurization of the hydraulic system).

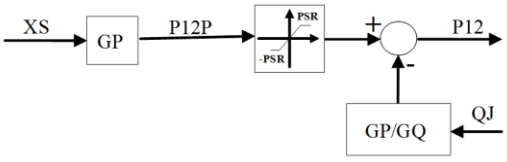

Figure 4 Nonlinear SV fluid-dynamics numerical model.

For this purpose, Figure 4 shows a possible variant (derived from the previously described model): it consists in the implementation of a saturation block that acts on the differential pressure developed through the relative gain.
In this way, it is possible to progressively improve the performance of the model by calculating the effects of the P_{SR} differential supply pressure. However, it should be noted that the SV model thus described presents a severe defect, underestimating the actuation speed in case of a fully opened valve: this is particularly noticeable when the valve reaches the saturation condition for small spool strokes (if compared with its maximum displacement X_{SM}).

4.1 FLUID DYNAMIC MODELS A, C1 AND C3

In previous works [8-9, 22-23], the authors proposed several simplified models intended to modify the formulation of the two gains shown in Eq. (1), to better take into account of peculiar effects such as pressure saturations, leakages and water hammers. Among these, the best results have so far been provided by type C models, which introduce pressure saturation downstream of the flow rate feedback node (closing the counteraction ring of the flow).

In general, the main advantage offered by the C type models previously proposed by the authors consists of the ability to take acceptably into account the effects of P_{12} limitations on the actuation rate, so obtaining a more proper value of the no-load actuation rate itself. On the contrary, the main shortcoming of these models is represented by the inability to simulate the temporary overload conditions, eventually affecting the motor element. The inaccurate evaluation of the overload conditions is generally not considered so important, and, vice versa, the best performance in the assessment of the speed of actuation of the motor (thus providing a more precise value of the velocity of actuation with no load) is significantly considered.
From the operational point of view, the main objective of these non-linear models was the combination of two opposite, and often antithetical, features: the maximum simplicity to represent the physical system (related to the reduced computational loads) and the high accuracy required (i.e. its fidelity in simulating the fluid-dynamic performance of the valve).
A first model, named Model C1 in [9], is shown in Fig. 5.
It includes leakage and variable P_{SR} computational algorithms and the flow feedback sum block, nevertheless being upstream the saturation block P_{SR}, has been displaced downstream the G_P one in order to use the invariant G_{PQ} block. In this way, the leakage feedback loop is fully located downstream the pressure saturation block, limited within the values ± P_{SR}.

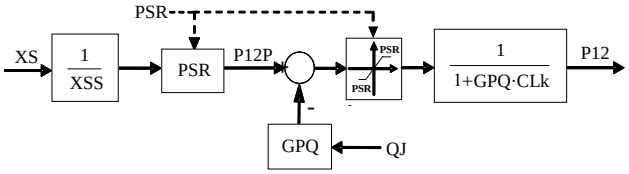

Figure 5 Model C1 block diagram [9].

Compared to the previous versions, the C1 model can simulate the effect of any changes in the P_{SR} during the simulation, evaluating (according to the proportionality assumption discussed above between G_P, G_Q and P_{SR}) the relative variable values of pressure gains and flow. Furthermore, the leakage feedback loop is analytically pre-solved to avoid computational instability problems.

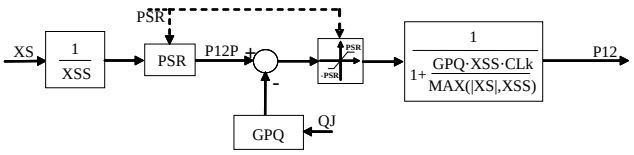

Figure 6 Model C3 block diagram [23].

Model C3 was initially introduced in [23]; as presented in Fig. 6, it takes into account the variable supply pressure and leakage acting among the control ports connecting the valve to the motor element. To account for supply pressure variation, we define $x_{SS} = P_{SR} / G_P$, where $P_{SR} = P_S - P_R$.
Despite being P_{SR} and G_P variable, x_{SS} is almost constant and only depends on the valve geometry. A leakage transfer function was added downstream the pressure saturation, with a variable gain to account for and avoid interaction with the saturation itself. Authors in [23] have provided a detailed explanation and derivation of the C3 model.
The resulting transfer function is:

$$P'_{12} = \begin{cases} -P_{SR}, & xP_{SR}\, x_S/x_{SS} - G_{PQ}Q_J < -P_{SR} \\ xP_{SR}\, x_S/x_{SS} - G_{PQ}Q_J, & -P_{SR} < xP_{SR}\, x_S/x_{SS} - G_{PQ}Q_J < P_{SR} \\ P_{SR}, & xP_{SR}\, x_S/x_{SS} - G_{PQ}Q_J > P_{SR} \end{cases}$$

$$P_{12} = P'_{12} \,/\, (1 + G_{PQ}\, x_{SS}\, C_{Lk} \,/\max(|x_S|, x_{SS})) \qquad (2)$$

where $G_{PQ} = G_P / G_Q$ and C_{Lk} is the ratio between the leakage flow Q_{Lk} the control pressure P_{12}. The model then employs a variable gain approach, which is intended to introduce the supply pressure variation into the leakage loop, as well as the information about the actual spool position. Specifically, the pressure gain is reduced for large spool displacements, in order to account for the limited available supply pressure.

5 PROPOSED FLUID-DYNAMIC VALVE MODEL

In this paper, the authors propose a new SFNM formulation (named C5 model), derived from the previous C-type models. Model C5 is intended to overcome the problems related to the interaction between the pressure saturation block and the

leakage feedback loop by modifying the formulation of the pressure/flow gain ratio G_{PQ} introduced in the C3 model. This is achieved by introducing a new equivalent spool position x_{St}, taking into account the effects of variable differential supply pressure P_{SR} and oil flow Q_J drained across the valve.
Model C5 is shown by the detailed block diagram of Fig. 7, and can be expressed with the following equations:

$$x_{St} = x_S - Q_J\, G_{PQ}\, x_{SS} / \max(P_{SR}, P_{vap}) \qquad (3)$$

$$P_{12} = x_{St}\, P_{SR} / (\max(|x_{St}|, x_{SS}) + C_{Lk}\, G_{PQ}\, x_{SS}) \qquad (4)$$

The location of the leakage loop entirely downstream or upstream the pressure saturation block, characterizing the previous C-type models, does not seem to give a sufficiently close representation of the actual physical phenomena.
In the intention of the authors, the model C5 (schematically shown in Fig. 7) should represent a development of these models capable of overcoming this drawback. It attempts to compute more efficiently and realistically the pressure gain effect in (pressure) saturation conditions by introducing a modified value of the spool displacement (called x_{St}) which is sensitive to variations in supply pressure and oil flow.
As reported in Eq. (3), the effect of the flow feedback reaction (due to the flow of oil Q_J crossing through the regulation ports of the valve) becomes more relevant as the supply pressure is reduced (up to the corresponding vapour tension value P_{vap}). As shown in the following section, this solution simulates more realistically the cases of high spool displacement but, as can be seen from Fig. 11, it is still unsatisfactory in fine regulation (i.e. for small spool openings around its centred position).

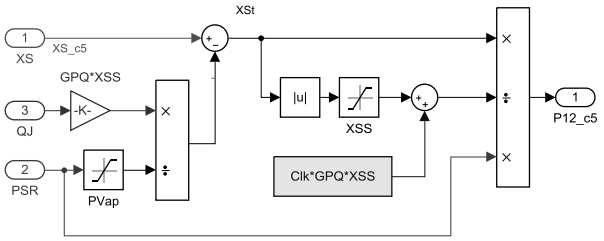

Figure 7 Model C5 block diagram [23].

6 SV FLUID-DYNAMIC CHARACTERISTICS P_{12} - X_S

A first evaluation of the said numerical models should be performed on the basis of the corresponding SV fluid-dynamic characteristics P_{12} - x_S, parameterized in Q_J.
The resulting diagrams show the differential pressure P_{12} acting on the motor element, for each value of P_{SR} and C_{Lk}, as a function of the displacement of the valve spool x_S, having the flow Q_J through the piston as a parameter.
The characteristics P_{12} - x_S for all the considered models have been computed referring to a SV featuring a value of $x_{SS} = 0.1$ mm, $G_{PQ} = 7.4 \cdot 10^{11}$ Pa·s/m^3, and $C_{Lk} = 2 \cdot 10^{-13}$ m^3/s/Pa, in presence of a supply pressure $P_{SR} = 20$ MPa.
The reference characteristic curve, obtained through the HF model, is shown in Fig. 2, and highlights the correct simulation of water-hammer, saturation and leakage.

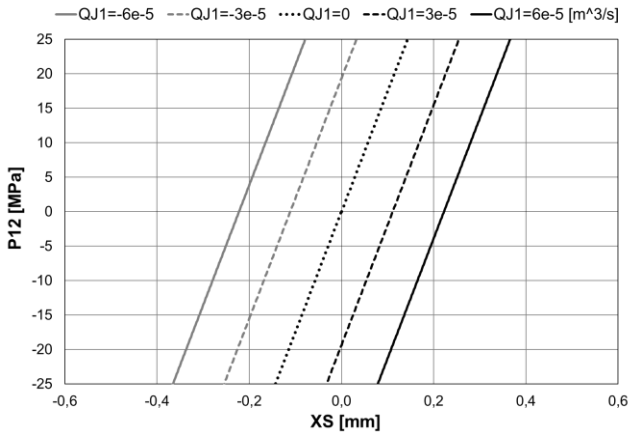

Figure 8 Differential pressure - spool position
SV characteristic P_{12}-X_S (model A)

Figure 8 shows the characteristic P_{12} - X_S calculate using the model A. In this case, according to what reported in the literature [9, 23], the inclination of the zero-flow curve is constant and lower than the G_P value, due to the effect of the leakages (C_{Lk} = $2 \cdot 10^{-13}$ m^3/s/Pa), as it appears correct, while no saturation is present, according to the model structure. Higher values of Q_J refer to lower P_{12} ones, like expected, not only in the present case but also in the following, as a consequence of the sign assumptions.
Figure 9 shows the characteristic P_{12} - X_S calculate using the model A. Also in this case, as widely reported in [9, 23], the slope of the zero-flow curve is constant but lower than the nominal GP value as a consequence of the leakages acting into the valve between spool and sleeve (C_{Lk} = $2 \cdot 10^{-13}$ m^3/s/Pa). Under saturation conditions, the P_{12} is calculated as invariant with respect to X_S for all Q_J values, as a consequence of the model structure. It represents the inability of the model to correctly calculate the high values reached by the differential pressure P_{12} in case of "water hammer", related to a sudden centering of the valve spool when the drive element is still rapidly moving. Under saturation conditions of P_{12}, the C1 model provides limit pressure values that, in modulus, are always lower than P_{SR}.

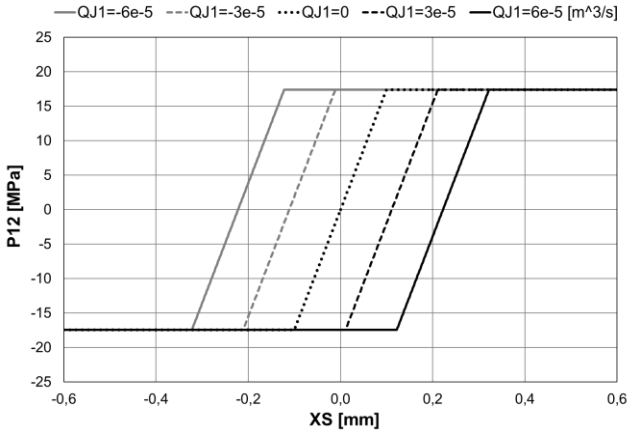

Figure 9 Differential pressure - spool position SV characteristic P_{12}-X_S (model C1)

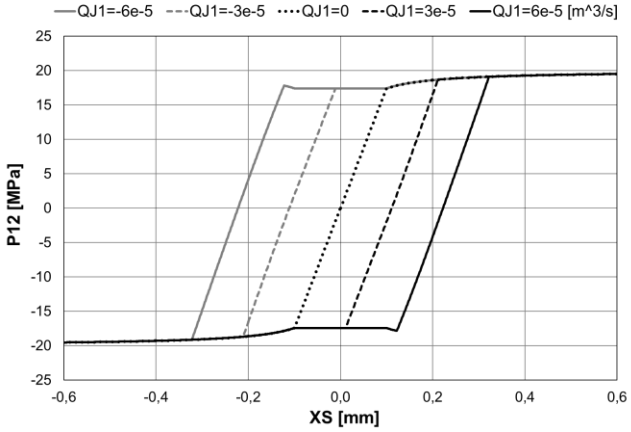

Figure 10 Differential pressure - spool position SV characteristic P_{12}-X_S (model C3)

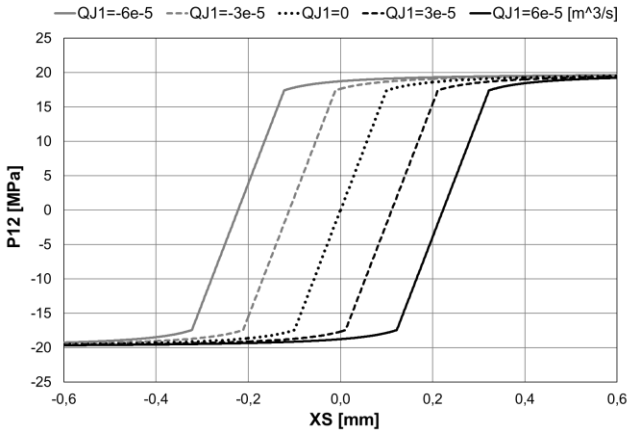

Figure 11 Differential pressure - spool position
SV characteristic P_{12}-X_S (model C5)

It can be explained considering that the block that calculates the effect of the hydraulic losses acts downstream of the pressure saturation one and therefore, for non-null C_{Lk} coefficients, it always makes its influence felt.
It should be also noted that under linear conditions, with the same spool displacement X_S, the highest values of differential pressure P_{12} are obtained for strongly negative Q_J flows (and vice versa); also this behavior can be explained by referring to the sign convention (Fig. 5).
As regards model C3 (Fig. 10), the slope of the zero-flow curve, in its central portion, is lower than the value of G_P, since it is modified by the effect of the leakage coefficient. As shown in [23], the model is not able to take correctly into account the effect of the saturation of P_{12}: in fact, for low values of spool displacement x_S, the algorithm calculates an anomalous evolution of the controlled pressure. This peculiar behaviour is due to the correction of the leakage coefficient being enabled only for $|x_S| > x_{SS}$, and is not representative of the real operation of the servo-valve. In particular, for $Q_J \neq 0$ and small spool displacements x_S (i.e. in water-hammer conditions), the experimentally detected differential pressure P_{12} is usually higher (and certainly not lower) than the saturation value P_{SR}.
The anomalous trend of the pressure curves of the C3 model is partly improved in the C5 model since the area in which the leakage coefficient correction is modified to be sensitive to the hydraulic flow Q_J. Figure 11 shows how the fluid-dynamic characteristic is acceptable for large spool displacements (i.e. $|x_s| >> x_{ss}$); however, the C5 model still fails to assess the effect of the water hammer accurately.

7 EHA TEST BENCH NUMERICAL RESULTS

The proposed simplified models are further tested by integrating them into a virtual test bench, which simulates a full position control electrohydraulic servoactuator.
In order to compare the behaviour of the different models and related computational algorithms concerning the fluid dynamics of the control valve equipping a hydraulic actuation servomechanism, a typical system was considered. Referring to the block diagram of Fig. 12, it mainly consists of a Power Control and Drive Unit (PCDU) and its control is performed by an Electronic Control Unit (ECU), closing the position control loop, calculating the instantaneous position error, and generating the reference current signal i_c by means of the controller. The PCDU contains the electro-hydraulic two-stage control SV and a hydraulic piston.
The actuator model takes into account the main electrical, hydraulic and mechanical characteristics of all the system components that are relevant to the purpose, including inertia, viscous and dry friction on the hydraulic piston, and a third order electromechanical model of the SV.

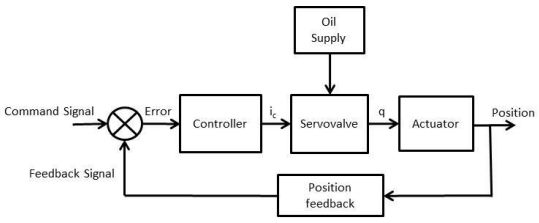

Figure 12 Block diagram of the EHA test bench.

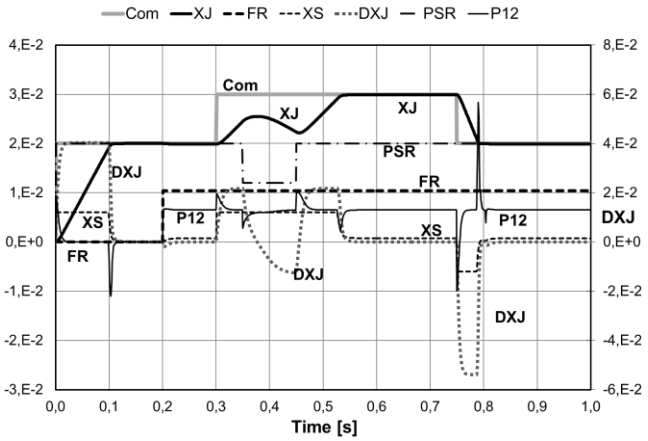

Figure 13 Test bench simulation with the HF model.

The simulations shown in Figures 13 to 17 represent the dynamic response of the EHA to a combination of position controls (*Com*), external loads (F_R) and variations in the hydraulic supply pressure (P_{SR}), for the different models of the second stage sliding spool valve. The input sequence was defined to highlight the performance of the proposed fluid dynamics models and their effect on the behavior of the simulation test bench [9, 23]. The response of the EHA testbench equipped with the HF model is shown in Fig. 13, as reference for the comparison with the simplified models.

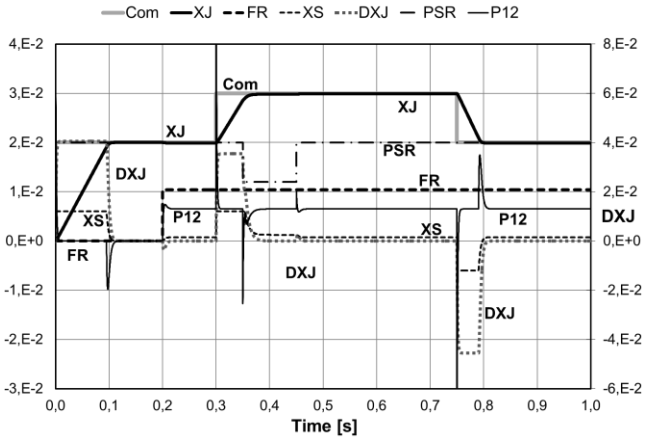

Figure 14 Test bench simulation with the A model.

Figure 14 shows the dynamic behavior of the EHA numerical testbench equipped with model A. The simulation of the actuation stroke without load is sufficiently accurate, despite the higher starting accelerations and lower stopping decelerations, as shown by the differential pressure P_{12}. Similar considerations apply to run under aiding load, while the opposing load run shows marked differences: according to model A, the effect of the opposite load on the actuation rate is underestimated and, when the supply pressure drops, the system back movement is absent. This behaviour is a consequence of the typical inability of model A to calculate the correct saturation value P_{12}. In loaded and motionless conditions the spool displacement is correctly not null, according to G_P value.

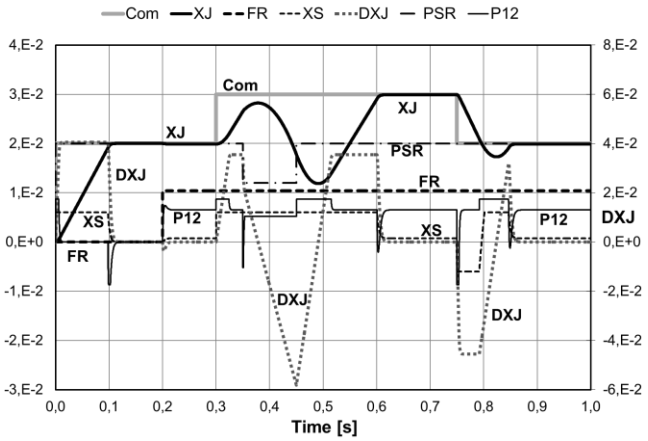

Figure 15 Test bench simulation with the C1A model.

Figure 15 shows the dynamic behavior of the EHA numerical testbench equipped with model C1. The no-load actuation stroke and the one with aiding load are simulated rather accurately, despite a lower stopping deceleration and slightly higher starting accelerations, as demonstrated by the behavior of P_{12}. The actuation stroke with opposing load reveals some notable discrepancies instead to the HD model: the load effect on the system actuation rate, in terms of reduction of the rate itself, is underestimated as in model A and, when the supply pressure drops; this backward movement of the system is overrated, calculating a wrong constant backward acceleration. Besides, the acceleration following a variation of the spool displacement maintains a constant value along a significant part of the acceleration transient, rather than the much more plausible asymptotic tendency reported in the HF model (similar to the first-order response due to a step input). The reason lies in the simple but partially unsatisfactory action of the P_{12} saturation block, contained in the numerical algorithm shown in Fig. 5. In these conditions, the results given by model C1 are unreliable (if compared with the surely more accurate model HF ones) and are emphasized by increasing C_{Lk} values.
Similar considerations concern the stop of the jack following the run with aiding load, which performs an incorrectly delayed and underdamped action.

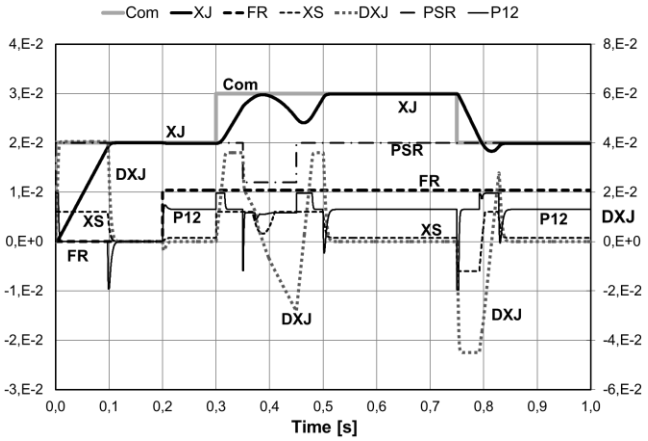

Figure 16 Test bench simulation with the C3 model.

Figure 16 shows the response of model C3; itis able to replicate with satisfying accuracy the behaviour of the HF model for the unloaded actuation (from 0 to 0.2 s) and the aiding load condition (at 0.75 s), despite a slightly higher starting acceleration and a lower stopping deceleration, due to the inability to account for the water hammer effect.
The simulation of the opposing load actuation (at 0.3 s) underestimates the effect of the external load, and at the supply pressure drop (0.35 s) the back movement is overestimated. This behaviour can be ascribed to the lack of water-hammer effect, i.e. when the valve passageways are closed, the differential pressure should grow higher than P_{SR} to resist an external load higher than the actuator stall force. Further, following a spool shift, the jack acceleration has an almost constant value (as shown by the constant slope of dx_J around 0.4 s), instead of the asymptotic trend of the HF model; the reason lies in the simple but partially unsatisfying action of the P_{12} saturation block.

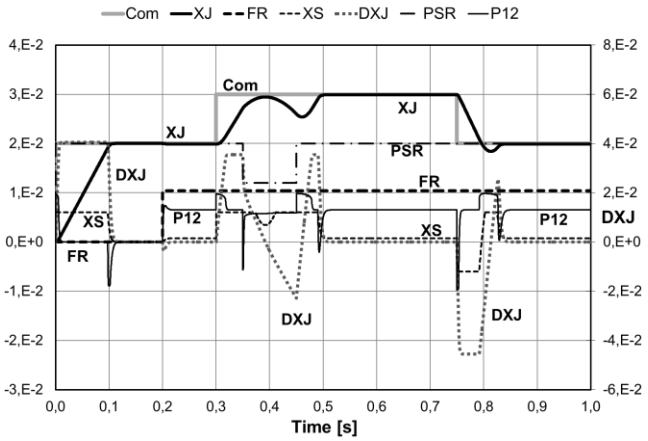

Figure 17 Test bench simulation with the C5 model.

Figure 17 shows the dynamic response of new model C5. The model behavior is almost identical to the previous case, meaning that model C5 shares the same issues of C3, and the correction made to the leakage loop is negligible in terms of dynamic response of the whole system.

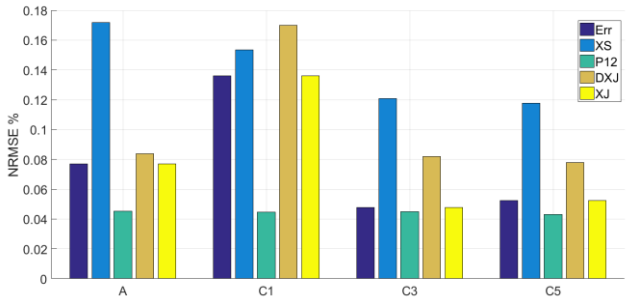

Figure 18 Normalized RMS error (NRMSE %).

The merits of the fluid dynamics models considered can be quantified by assessing their consistency with the HF model. To this purpose, Fig. 18 shows the NRMSE % values calculated by comparing the temporal responses of the HF model with those of the simplified models.

7 CONCLUSIONS

The analysis of the considered fluid-dynamic numerical models clearly shows the few advantages and the critical shortcomings affecting the proposed simplified algorithms.
Dynamic transients (accelerations, decelerations), water hammer and transient pressure conditions are overrated or underestimated, as a function of the particular operating condition; at the moment it is not yet available a completely satisfactory servovalve simplified model, based only on easily measurable parameters, able to combine adequate precision and limited computational complexity.
In particular, the proposed C5 model is not capable of overcoming the issues of the other C-type models, from which it was derived. In this regard, the authors think that further studies are needed to develop more efficient algorithms capable of performing acceptable simulations in all possible working conditions.

LIST OF SYMBOLS

C_{Lk}	Leakage coefficient
Com	Servomechanism position command
dx_J	Motor element velocity
ECU	Electronic Control Unit
EHA	Electrohydraulic Actuator
F_R	Load acting on the motor element

G_P	Pressure gain
G_Q	Flow gain
G_{PQ}	Pressure to flow gain ratio G_P/G_Q
i_c	Reference current signal of the valve
P_{12}	Actual differential pressure
P_{12P}	Zero-flow controlled differential pressure
PCDU	Power Control and Drive Unit
P_{SR}	Supply/return differential pressure
P_{vap}	Hydraulic fluid vapour tension value
Q_{Lk}	Leakage flow
Q_J	Working flow
SFNM	Simplified Fluid-dynamic Numerical Model
SV	Servovalve
x_J	Motor element position
x_S	Spool displacement
x_{SM}	Spool end of travel displacement
x_{SS}	P12P saturation spool displacement

ACKNOWLEDGEMENTS

The authors wish to extend a heartfelt thanks to Prof. Lorenzo Borello for his valuable teachings and for his support in the conception and development of this research.

REFERENCES

[1] De Martin A., Chiavaroli P., Evangelista G., Jacazio G. and Sorli M., Real Time Loading Test Rig for Flight Control Actuators under PHM Experimentation. *Proc. of the ASME 2018 International Mechanical Engineering Congress and Exposition*, 2018.

[2] Henninger D., Zopey A., Ihde T. and Mehring C., High-Fidelity 1D Dynamic Model of a Hydraulic Servo Valve Using 3D Computational Fluid Dynamics and Electromagnetic Finite Element Analysis. International Journal of Mechanical and Mechatronics Engineering, Vol. 11, Nno. 8, pp. 1476-1482, 2017.

[3] Chen Q. and Stoffel B., CFD Simulation of a Hydraulic Servo Valve with Turbulent Flow and Cavitation. *ASME/JSME 2004 Pressure Vessels and Piping Conference*, 2004.

[4] Borello L., Dalla Vedova M.D.L., Jacazio G. and Sorli M., A prognostic model for electrohydraulic servovalves. *Annual Conference of the Prognostics and Health Management Society (PHM 2009)*, 2009.

[5] Dalla Vedova M.D.L., Maggiore P. and Pace L., Proposal of Prognostic Parametric Method Applied to an Electrohydraulic Servomechanism Affected by Multiple Failures. *WSEAS Trans. on Environment and Development*, Vol. 10, pp. 478-490, 2014.

[6] De Martin A., Dellacasa A., Jacazio G. and Sorli M., High-Fidelity Model of Electro-Hydraulic Actuators for Primary Flight Control Systems. *BATH/ASME Symposium on Fluid Power and Motion Control*, 2018.

[7] Kim D.H. and Tsao T.C., A Linearized Electrohydraulic Servovalve Model for Valve Dynamics Sensitivity Analysis and Control System Design. *ASME Journal of Dynamic Systems, Measurement, and Control*, Vol. 122, No. 1, pp. 179-187, 2000.

[8] Borello L., Villero G., Confronto fra modelli semplificati di valvole di comando. *XI A.I.D.A.A. National Congress*, Forlì (Italy), 14-18 October 1991.

[9] Alimhillaj P., Borello L. and Dalla Vedova M.D.L., Proposal of Innovative Fluid Dynamic Nonlinear Servovalve Synthetic Models. *International Journal of Mechanics and Control*, Vol. 14, No. 2, pp. 39-49, December 2013.

[10] Borello L., Villero G., Modello matematico completo di valvole di commando per azionamenti idraulici. *NT Tecnical & Tecnologia*, No. 1, pp. 39-47, 1991.

[11] H. E. Merritt, *Hydraulic Control Systems*, John Wiley and Sons Inc, 1967.

[12] T.J. Viersma, *Analysis, synthesis and design of hydraulic servosystems and pipelines*, Elsevier, 1980.

[13] Urata E., Study of magnetic circuits for servovalve torque motors. *Bath workshop on power transmission and motion control*, Bath (UK), pp. 269-282, 2000.

[14] Urata E., Study on Leakage Flux from Servovalve Torque Motors. *The Seventh Scandinavian Int. Conf. on Fluid Power*, Linköping, Vol. 1, pp. 51-66, 2001.

[15] Urata E., Influence of fringing on servovalve torque-motor characteristic. *Proc. Fifth JFPS Intl. Symp. on Fluid Power*, Nara, Vol. 3, pp.769-774, 2002.

[16] Urata E., Static Stability of Toque Motors. *The Eighth Scandinavian Intl. Conf. on Fluid Power*, Tampere, Finland, pp. 871-885, 2003.

[17] Urata E., Influence of eddy current on torque-motor dynamics. *4th IFK Workshop*, Dresden, Germany, pp. 71-82, March 2004.

[18] Urata E., One degree of freedom model for torque motor dynamics. *International Journal of Fluid Power*, Vol. 5, No. 2, pp. 35-42, 2004.

[19] Urata E., Influence of asymmetry of air-gap in servovalve torque motor. *The Ninth Scandinavian Int. Conf. on Fluid Power*, Linkoping, Sweden, 2005.

[20] Jia W. and Yin C., CFD Simulation with Fluent and Experimental Study on the Characteristics of Spool Valve Orifice. *2nd International Conference on Computer Engineering and Technology - IEEE*, Chengdu, China, 2010.

[21] Pan X., Wang G. and Lu Z., Flow field simulation and a flow model of servo-valve spool valve orifice. *Energy Conversion and Management*, No. 52, pp. 3249-3256, Elsevier, 2011.

[22] Borello L. and Dalla Vedova M.D.L., Pseudo-dynamic simulation method solving hydraulic stationary problems. *International Journal of Mechanics and Control*, Vol. 8, No. 2, pp. 4-52, 2007.

[23] Alimhillaj P. and Dalla Vedova M.D.L., Study of new fluid dynamic nonlinear servovalve numerical models for aerospace applications. *2nd European Conference on Electrical Engineering & Computer Science (EECS 2018)*, Bern (CH), 2018.